Reprinted from *Agronomy Journal*
Vol. 79, No. 6

In Situ Nuclear Magnetic Resonance Imaging of Roots: Influence of Soil Type, Ferromagnetic Particle Content, and Soil Water

Hugo H. Rogers and Paul A. Bottomley

In Situ Nuclear Magnetic Resonance Imaging of Roots: Influence of Soil Type, Ferromagnetic Particle Content, and Soil Water[1]

Hugo H. Rogers and Paul A. Bottomley[2]

ABSTRACT

The paucity of root information combined with the difficulty in obtaining it make new approaches imperative. The observation of roots is essential to the understanding of plant growth and productivity. Proton (^1H) nuclear magnetic resonance (NMR) imaging offers a noninvasive method for the study of both root morphology and function in situ. Herein, NMR imaging of plant root systems was evaluated for southeastern U.S. agricultural soil series from 30 different sites, and eight common artificial soil substrates, as a function of soil type, ferromagnetic particle content, and soil water, using a 1.5-tesla medical research NMR imaging system and *Vicia faba* L. seedlings grown in the soils. Roots of about 1 mm in diameter and 1-mm-diam capillaries of water were undetectable by NMR imaging and conventional NMR in soils with ferromagnetic particle contents of greater than about 4% by weight. Below 4%, ferromagnetic particle content did not correlate well with NMR image quality, but the presence or absence of NMR signals from water-containing capillaries embedded in soil samples in a conventional NMR experiment reliably reflected soil suitability for NMR root imaging. Images of seedlings in four of the artificial soils (perlite, Ottawa sand, peatlite, and peat) and seven of the native soils (Wynnville fine sandy loam, Lucy loamy sand, Dothan sandy loam, Lakeland sand, Kinston loamy sand, Blanton loamy sand, and Eustis fine sandy loam) showed excellent spatial resolution and accurate reproduction of the root systems when they were extricated from the soils. However, the results from three of the artificial soils (perlite, Ottawa sand, and peat) were significantly compromised by background NMR signals that derived from soil water. In the seven native soils, soil water to near saturation was rendered essentially invisible by the NMR imaging sequence employed, thereby demonstrating excellent root-to-soil image contrast. Several root pathologies apparent in the images were identified. The results reveal that ^1H NMR imaging is a practical tool for the nondestructive, noninvasive investigation of plant root systems in many natural agricultural soils at virtually any stage of a water stress cycle.

Additional index words: Roots, Root research methods, In situ root observation, Soil magnetic properties, Soil NMR properties.

ROOT structure and dynamic response to different soil conditions are of pivotal importance for the evaluation of plant growth and productivity. Traditional manual techniques for studying root morphology and function are often destructive, tedious, and inaccurate. Therefore, the need for new nondestructive research technologies to address rhizosphere dynamics is urgent and widely stressed (1,2,6). New approaches include neutron radiographic imaging of root systems (17,19), the use of color video cameras in mini-rhizotrons (18), root measurements with the image-analyzing computer (11), porous membrane root cultures in the field (5), modified weighing lysimeters for providing profiles of root density and water extraction (7), herbicide banding to screen root genotypes in the field (14), and x-ray computed tomography (9). However, none of these techniques provides noninvasive, nondestructive access to information about root water and its transport within the living plant.

We recently investigated the application of proton (^1H) nuclear magnetic resonance (NMR) imaging to plant root systems in situ using undisturbed *Vicia faba* L. (broad bean) seedings grown in several different artificial soil media (4,15). Since the signal intensity in NMR images is most sensitive to the mobility of protons with a high degree of molecular-level mobility such as those of hydrogen in water, NMR images of plant root systems represent maps of water distribution in roots and hypogeal cotyledons, thereby delineating the morphology of the root system. Furthermore, sequential images can reveal changes in image intensity that reflect water transport and loss in root systems in response to various plant stresses. Thus, NMR imaging provides a currently unique, noninvasive means of studying root morphology in situ and directly monitoring hydrodynamic root function in stressed environments.

Nuclear magnetic resonance employs static and radiofrequency (RF) magnetic fields to align and excite, respectively, magnetic resonance in ^1H nuclei (10). Therefore, NMR is sensitive to the presence of ferromagnetic particles occurring naturally in soil media, which can disturb the applied magnetic field locally, and thereby distort or destroy the local NMR imaging information. Similarly, the presence of good RF electrical conduction pathways in soil media could prevent adequate penetration of the RF excitation and detection fields, resulting in NMR image attenuation or even a complete loss of the NMR signal intensity. Moreover, the presence of soil water, even at the lowest concentrations studied, can easily represent the dominant source of water in any integrated root-bearing soil cross section, and dominate or completely overwhelm NMR signal contributions from water in small roots.

To investigate the range of potential applications of ^1H NMR imaging in plant root systems and to assess the impact of soil magnetic properties and water content on this new technology, we evaluated plant root NMR imaging in 30 different natural soil samples and eight different artificial soil media as a function of soil type, ferromagnetic particle content, and soil water.

MATERIALS AND METHODS

Thirty different soil samples from 24 series representing a broad range of southeastern U.S. agricultural soils and including several soils with low iron contents were collected in 60-L drums from Auburn University experimental agricultural substations and other defined sites distributed throughout Alabama. In addition, eight common, commercially available artificial soil substrates were acquired. A descriptive list of these soils appears in Table 1. Each soil sample was air-dried, homogenized by mixing, the dry density and water content measured gravimetrically (oven-dry weight basis; 105°C to constant weight, usually 72 h), and the ferromagnetic particle content determined by sieving 5-L aliquots through a 2-mm screen onto a 0.23-tesla magnet

[1] Contribution from the Natl. Soil Dynamics Lab., USDA-ARS, P.O. Box 792, Auburn, AL 36831, and General Electric Corp. Res. and Dev. Ctr., P.O. Box 8, Schenectady, New York 12301. Received 6 Oct. 1986.

[2] Plant physiologist and NMR physicist, respectively.

Published in *Agron. J.* 79:957–965(1987).

Table 1. Description and physical properties of artificial and native soils studied, ranked by magnetic fraction.

Material	Description	Magnetic fraction	NMR linewidth†	NMR intensity†	Dry density	Soil water‡
		%	Hz		g m^{-3} × 10^{6}	g kg^{-1}
Artificial media						
Vermiculite	Terra-Lite: W.R. Grace and Co., Cambridge, MA	21.9	--	--	0.2	9(1430)
Perlite	Terra-Lite	1.2	90[58]	0.44[0.50]	0.1	5(2660)
Sand	Medium grain, construction grade	1.2	--	--	1.1	1(9)
Fritted Clay	Absorb-N-Dry: Balcones Mineral, Faltonia, TX	0.5		--	0.6	54(280)
Potting Soil	K-Mart Ready-to-Use: Old Fort Industries, Fort Wayne, IN	0.3		--	0.2	43(1050)
Ottawa Sand	A.F.S. Testing Sand 50-70: Ottawa Silica Co. Ottawa, IL	0.1	38[38]	0.45[0.28]	1.7	0(44)
Peatlite	Pro-Mix: Premier Brands, New Rochelle, NY	0.1	83[38]	0.56[0.16]	0.1	107(190)
Peat	Premier Sphagnum Peat Moss: New Rochelle, NY	0.00	12[19]	0.77[0.77]	0.1	138(1510)
Soil series						
Decatur clay loam	Clayey, kaolinitic, thermic Rhodic Paleudults	39.5	--	--	1.1	19
Davidson clay	Clayey, kaolinitic, thermic Rhodic Paleudults	37.5	--	--	1.1	23
Decatur silt loam	Clayey, kaolinitic, thermic Rhodic Paleudults: first site	30.9	--	--	1.1	19
Decatur silt loam	Clayey, kaolinitic, thermic Rhodic Paleudults: second site	12.5	--	--	1.0	18
Oktibbeha clay	Very fine, montmorillonitic, thermic Vertic Hapludalfs	9.8	--	--	1.2	36
Congaree clay loam	Fine-loamy, mixed, nonacid, thermic Typic Udifluvents	7.5	--	--	1.1	19
Ruston fine sandy loam	Fine-loamy, siliceous, thermic Typic Paleudults	6.9	--	--	1.0	10
Wynnville fine sandy loam	Fine-loamy, siliceous, thermic Glossic Fragiudults: first site	3.8	--	--	1.1	7
Stough loam	Coarse loamy, siliceous, thermic Fragiaquic Paleudults	3.8	--	--	0.9	2
Eustis fine sandy loam	Sandy, siliceous, thermic Psammentic Paleudults: first site	3.7	--[56]	--[0.50]	1.2	5
Cahaba sandy loam	Fine-loamy, siliceous, thermic Typic Hapludults	3.4	--	--	1.2	6(9)
Wynnville fine sandy loam	Fine-loamy, siliceous, thermic Glossic Fragiudults: second site	2.8	44[44]	0.33[0.33]	1.1	6(24)
Vaiden silty clay	Very fine, montmorillonitic, thermic Aquentic Chromuderts	2.2		--	1.1	51
Eustis fine sandy loam	Sandy, siliceous, thermic Psammentic Paleudults: second site	1.8	43[44]	0.43[0.39]	1.3	4(19)
Sharkey silty clay	Very fine, montmorillonitic, nonacid thermic Vertic Haplaquepts	1.7		--	1.0	68
Sumter silty clay loam	Fine-silty, carbonatic, thermic Rendollic Eutrochrepts	1.5	--	--	0.9	72
Hiwassee clay	Clayey, kaolinitic, thermic Typic Rhodudults	1.4	--	--	1.0	33
Wynnville fine sandy loam	Fine-loamy, siliceous, thermic Glossic Fragiudults: third site	1.4	--[77]	--[0.29]	1.0	9
Wilcox clay	Fine, montmorillonitic, thermic Vertic Hapludalfs	1.1	--	--	0.9	85
Wagram loamy fine sand	Loamy, siliceous, thermic Arenic Paleudults	1.0	--	--	1.2	3
Lucy loamy sand	Loamy, siliceous, thermic Arenic Paleudults	0.9	28[28]	0.21[0.21]	1.2	5(80)
Dothan sandy loam	Fine-loamy, siliceous, thermic Plinthic Paleudults: first site	0.9	28[28]	0.70[0.70]	1.3	4(14)
Lakeland sand	Thermic, coated Typic Quartzipsamments	0.7	--	--	1.4	2(21)
Blanton loamy sand	Loamy, siliceous, thermic Grossarenic Paleudults: first site	0.7	--[45]	--[0.45]	1.4	3
Hiwasse sandy loam	Clayey, kaolinitic, thermic Typic Rhodudults	0.7	--	--	1.3	9
Dothan sandy loam	Fine loamy, siliceous, thermic Plinthic Paleudults: second site	0.5	47[46]	0.49[0.42]	1.2	4
Kinston loamy sand	Fine-loamy, siliceous, acid, thermic Typic Fluvaquents	0.4	83[83]	0.69[0.69]	1.1	10(33.113)
Blanton loamy sand	Loamy, siliceous, thermic Grossarenic Paleudults: second site	0.4	--	--	1.3	3(43)
Houston clay	Very fine, montmorillonitic, thermic, Typic Chromuderts	0.3	--	--	1.0	80(193)
Norfolk sandy loam	Fine-loamy, siliceous, thermic Typic Paleudults	0.2	--[58]	--[10.00]	1.3	7

† NMR measurements from 1.2-mm water-containing capillary embedded in a 30-mm-diam sample tube of soil media. Bracketed figures represent NMR measurements from magnetically screened soil media (ferromagnetic particles removed). Blanks represent no detectable signal. NMR intensity is relative to the signal detected from the capillary removed from the soil which assumed a value of 1. The NMR linewidth in the absence of soil was 8 Hz.

‡ Gravimetric, oven-dry weight basis. First value obtained at time of magnetic fraction determination; figures in parentheses obtained at time of imaging study (Fig. 1–4).

with a 0.06-m^2 pole-face inclined at 45°. The ratio of the mass of magnetic material that accumulated on the magnet to the total aliquot mass following repeated screening of aliquots provided a measure of ferromagnetic particle content, and was denoted by the magnetic fraction, M. Removal of magnetic particles adhering to the magnet between each screening was facilitated by use of a plastic film that covered the magnet.

The suitability of soil samples for in situ plant root NMR imaging was assessed by conventional NMR spectroscopy without NMR imaging, and by direct NMR imaging of root-bearing media. Thorough discussions of both NMR spectroscopy and NMR imaging are available (8,10,13,16,20). All ^{1}H NMR studies were performed at 64 MHz using a 1.5-tesla, 1-m bore General Electric medical research NMR imaging system with a 140-mm-diam NMR receiver coil (3), located at the General Electric Corporate Research and Development Center in Schenectady, NY. In the conventional NMR examination, glass capillaries 50 mm long by 1.2-mm inner diameter were filled with water and embedded vertically in plastic sample tubes containing magnetically sieved and unsieved (natural) soil media. The plastic sample tubes measured 30 mm in diameter by 80 mm in height. The imbedded capillaries simulated roots of similar diameter.

Nuclear magnetic resonance was excited and detected from the water in the capillaries in the dried soil samples, and the

integrated NMR signal intensities and full-width-half-maximum (fwhm) linewidths of the resonances were recorded. Resonance linewidths, $\Delta\nu$, are related to the local magnetic field inhomogeneity, ΔH, across the sample via

$$\Delta\nu = (\pi T_2)^{-1} + \gamma\Delta H(2\pi)^{-1},$$

where T_2 is the NMR spin-spin relaxation time of the water protons,[3] and γ is the nuclear gyromagnetic ratio of ^1H. The comparison of the water resonance linewidths recorded with the capillary embedded in the soil and those recorded with the capillary alone thus provided a direct measure of the additional static field inhomogeneity introduced by the soil. Similarly, the integrated signal intensity of the water resonance provided some indication of the ability of the RF magnetic field to penetrate soil samples. However, the signal intensity is not entirely independent of linewidth measurements since extremely broad resonances that are indistinguishable from the baseline also register an intensity of essentially zero. Nevertheless, the NMR signal intensity from inside a soil sample relative to that achievable in the absence of soil is obviously an important indicator of the suitability of the soil media for NMR imaging.

Plant root NMR imaging studies utilized *Vicia faba* L. seedlings grown singly in 150-mm plastic pots (white, opaque) each containing one of the artificial soil media and a subset of the unsieved natural soil series that was not magnetically screened. Selection of the latter was based on the results of the magnetic fraction and conventional NMR studies. Four plants were produced for each soil type.

Study plants were pregerminated in germination paper wetted with 10^{-5} *M* $CaCl_2$ and transplanted at 3 days into the 150-mm pots. All seedlings were grown for 30 days in a greenhouse at the National Soil Dynamics Laboratory, Auburn, AL, under relatively dry conditions to avoid waterlogging which could kill the roots, but were rewatered from the bottom at the first sign of stress (15 Oct.–15 Nov. 1985). Plants were transported by commercial airline to NMR facilities in New York. Light was supplied to plants outside the NMR machine by three 850-W quartz iodide lamps (Hedler, Turbo-Lux Super Safe 1250; Wolf Camera Supply, Inc., Atlanta, GA) and within the magnet bore during imaging experiments by two 100-W, 12-V DC quartz-iodide lamps (Sylvania EFP; E. Sam Jones Distribution, Atlanta, GA) in nonmagnetic housings. Both types of lamps provided a suitable spectrum for plant growth, with an incident photon flux density of 2000 μmol photon m^{-2} s^{-1}. Air temperature and relative humidity were maintained at 26.5°C and 38%, respectively, in the NMR laboratory. The potted plants were oriented vertically in the NMR receiver coil in the center of the bore of the imaging magnet.

Nuclear magnetic resonance imaging was performed using a conventional 256- by 256-point spin-warp spin-echo NMR imaging sequence, with 0.56- by 0.56-mm spatial resolution in the horizontal and vertical directions of the imaging plane. Finer spatial resolution is achievable, albeit at the expense of a reduced field-of-view or an increased scan time, or both, all other parameters being equal. Spatial selection in the third dimension was omitted so that roots traversing laterally would appear as continuous traces. The delay time between the initial $\pi/2$ NMR excitation pulse and the NMR spin-echo signal was 20 ms, and the NMR pulse sequence repetition period was 1.0 s. The former image timing parameter discriminated against those ^1H NMR signals in the soil-root system for which NMR T_2 values were less than 20 ms. Choice of the 1.0-s sequence repetition period resulted in some minor attenuation of the root NMR signal by a saturation factor of about 0.90 ± 0.05 due to NMR spin-lattice relaxation (T_1) processes.[4] Scan times were 8.5 min per image.

After imaging, soil samples were collected from pots into soil cans for soil water determinations (at the Auburn lab after main study). Root systems were then carefully extricated from the soil, washed, and photographed for comparison with the NMR images. The nature of *V. faba* roots at this stage makes them easily retrievable from the soil. Root systems that appeared in images as abnormal or diseased were examined and pathogens identified where possible. To further investigate the NMR appearance of soil water in images, several other non-plant-bearing containers were prepared with separated layers of soil media possessing different water contents.

RESULTS

Magnetic fractions, dry densities, water contents measured at the time of magnetic fraction determination and at the time of NMR imaging experiments, fwhm NMR linewidths, and integrated NMR signal intensities from the conventional NMR study are all tabulated in Table 1. Native and artificial soils with magnetic fractions $M \geq 4\%$ produced NMR signals from the 1.2-mm capillaries that were undetectable in the conventional NMR study, regardless of whether or not the soils were magnetically screened. Soils with $M < 4\%$ either exhibited improved NMR properties (reduced linewidth or increased signal intensity, or both) following magnetic screening, as in perlite, peatlite, Eustis fine sandy loam, Wynnville fine sandy loam, Blanton loamy sand, and Norfolk sandy loam soils, or showed essentially no change, as in the remaining soils. Note that many soils exhibiting magnetic fractions $M \leq 1\%$ were not conducive to NMR examination by conventional means.

Nuclear magnetic resonance images of *V. faba* in unscreened artificial soil substrates are shown in Fig. 1, ordered as listed in Table 1. All seedlings were imaged at about 30 days after planting, except for Fig. 1E which contained two seedlings 7 days after planting. All artificial soil systems exhibited detectable ^1H NMR signals from roots in images, including those soils that gave null results by conventional NMR. However, severe image distortion and apparently random disappearances of NMR signal from roots in vermiculite and sand are evident in Fig. 1A and Fig. 1C. Less severe image distortion and signal loss are apparent for fritted clay in Fig. 1D and for potting soil in Fig. 1E. Indeed, comparison of these images with the washed extricated root systems indicated that roots of less than 1.0-mm diameter were typically unobservable in images of the artificial substrates; this is consistent with the results from the conventional NMR test.

In Fig. 1, seedlings in perlite (B), Ottawa sand (F),

[3] T_2 is the characteristic time constant for any net nuclear magnetization that is present in the plane transverse to the direction of the main applied field to decay away. Since this decay is hastened by local *static* magnetic field inhomogeneities at the molecular level, short T_2 values are generally characteristic of more rigidly bound systems such as water adsorbed onto polar surfaces or in hydrogen-bonded structures. The T_2 of free water is ~2 s.

[4] T_1 [$\leq T_2$] is the characteristic time constant for the nuclear magnetization to align with the main applied magnetic field. The rate at which alignment occurs depends on the intensity of molecular-level magnetic field *fluctuations* at the NMR frequency: the greater the motion at the NMR frequency, the greater is the relaxation rate, and the shorter is the T_1 value. The T_1 of free water is ~2 s [~T_2].

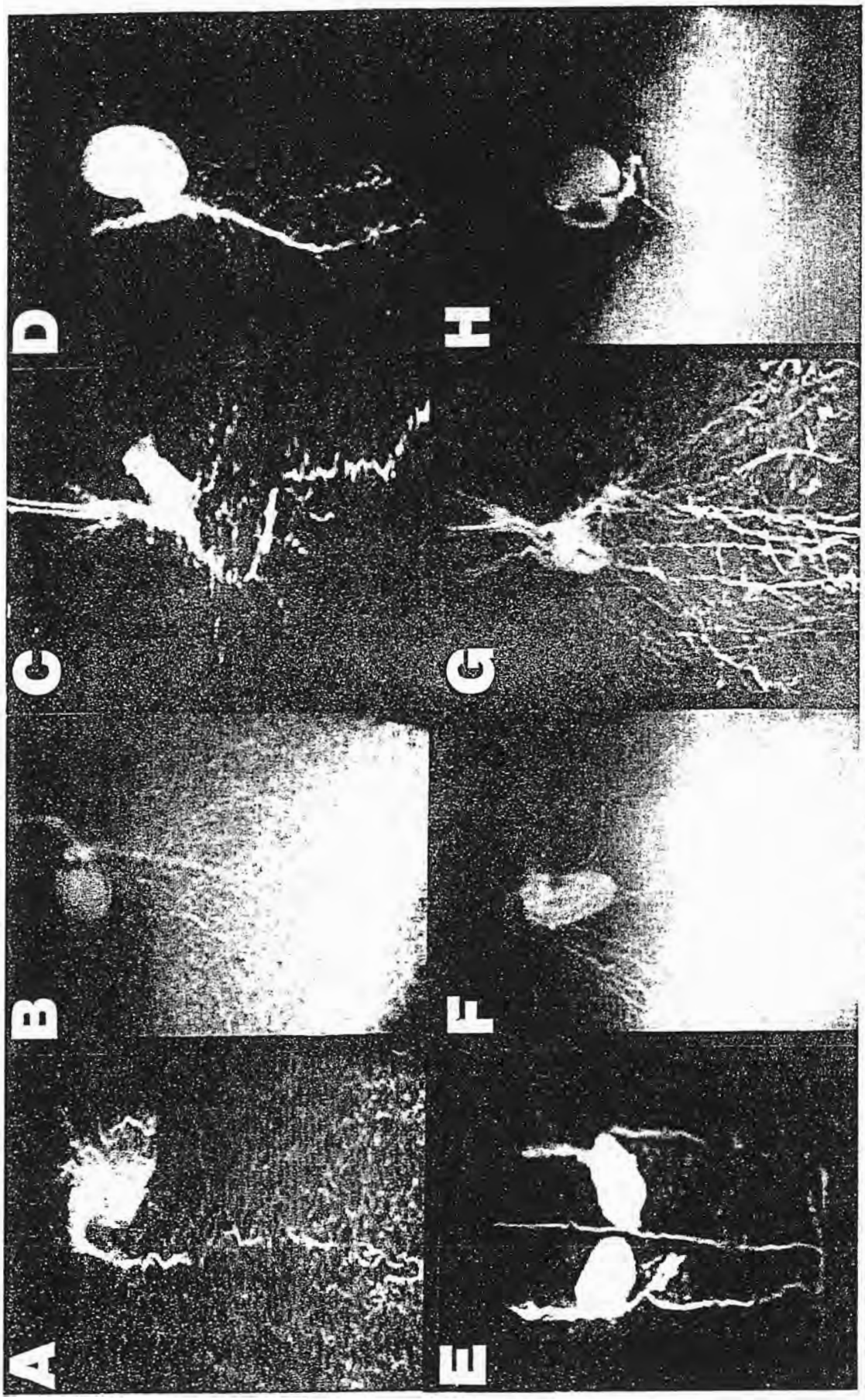

Fig. 1 ^{31}P NMR images of *V. faba* root systems in vermiculite (A), perlite (B), construction grade sand (C), fritted clay (D), potting soil (E), Ottawa sand (F), peatlite (G), and peat (H) as described in Table 1. All seedlings are 30 days old except for potting soil (E), which contains two seedlings 7 days after planting, separated by a 90- by 1.2-mm inner diameter straight capillary, which appears as a crooked vertical bright line at the center. Hypogeal cotyledons appear as bright ovals towards the top center of images, stems emerge vertically upwards, and the root systems diverge downwards. The soil-air interfaces are just above the cotyledons. Bright background signals in B_1 F, and H derive from soil water. (Scale 1:1.7.)

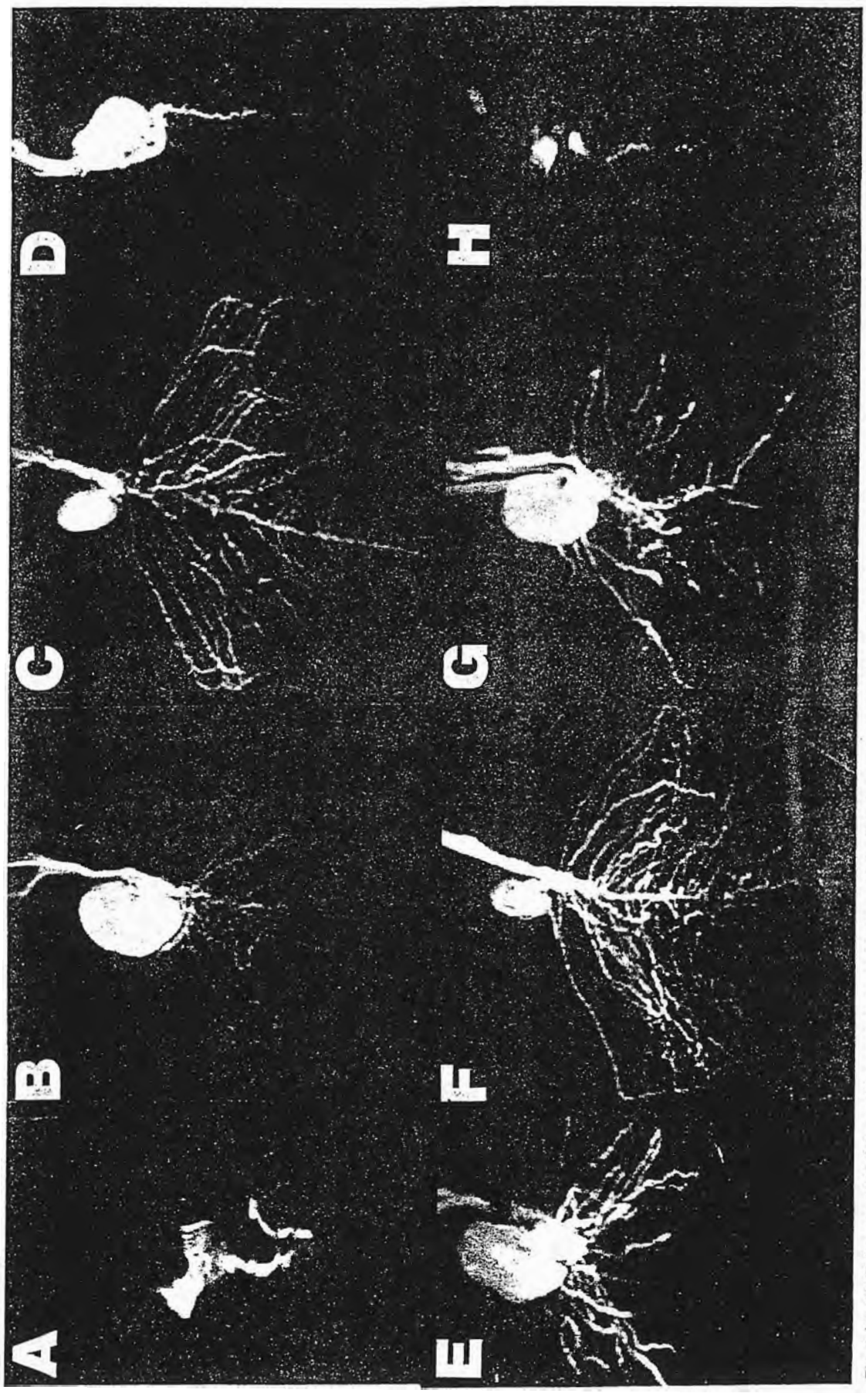

Fig. 2 ^{1}H NMR images of *V. faba* seedling root systems, 30 days old, in Cahaba sandy loam (A), Wynnville fine sandy loam (B), Lucy loamy sand (C), Dothan sandy loam (D), Lakeland sand (E), Kinston loamy sand (F), Blanton loamy sand (G), and Houston clay (H) soils, as described in Table 1. Soil water contents are 9, 24, 80, 14, 21, 33, 43, and 193 g kg^{-1}, respectively. Hypogeal cotyledons appear as bright ovals in B through G; stems ascend and root systems descend. Soil-air interfaces occur just above the cotyledons. (Scale 1:1.7.)

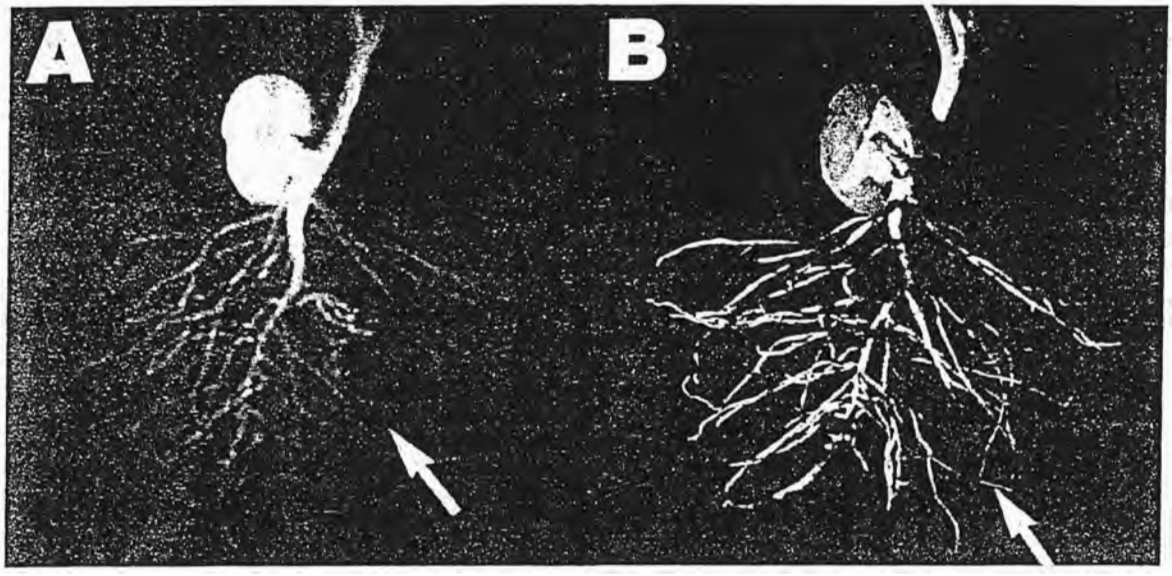

Fig. 3 ^{1}H NMR image of a 30-day-old *V. faba* seedling root system in Eustis fine sandy loam (A) with a 19 g kg^{-1} soil water content, compared to a photograph of the extricated washed seedling (B). Root structures as small as about 0.3 mm can be identified in images (white arrows). (Scale 1:1.7.)

and peat (H) exhibit dominant bright background signals that were distributed uniformly throughout the pots and attributable to soil water. Although both perlite and peat possessed soil water contents in seedling pots of greater than 100% (Table 1), so did potting soil (Fig. 1E) whose NMR image reveals a negligible soil water background. Conversely, the soil water content of the Ottawa sand pot with a strong background signal was 44 g kg^{-1}, greater than that measured for construction grade sand at 9 g kg^{-1} exhibiting little background signal. Thus, soil water content alone does not appear to be a good predictor of the presence or absence of background signals from soil water in plant root ^{1}H NMR images. The mottled appearance of the hypogeal cotyledon in Ottawa sand (Fig. 1F) corresponds to internal necrotic zones caused by *Corynebacterium*.

Figure 2 shows images of 30-day-old *V. faba* seedlings undisturbed in native Cahaba sandy loam, Wynnville fine sandy loam, Lucy loamy sand, Dothan sandy loam, Lakeland sand, Kinston loamy sand, Blanton loamy sand, and Houston clay soils, respectively. Figure 3 compares an in situ root image in Eustis fine sandy loam with a photograph of the extricated washed root system. These soil media were chosen for their low magnetic fractions (<4%) or their ability to provide a measurable NMR signal in the conventional NMR experiment, or both. Since our aim in studying native soils was to identify naturally occurring soil media that are suitable for root imaging investigations, and since magnetic screening did not guarantee improved suitability of soils for NMR studies (Table 1), plant root imaging was performed only with unscreened soil media.

The images of roots in Cahaba sandy loam (Fig. 2A) and Houston clay (Fig. 2H) soils show severe distortions and disappearances of NMR signal from roots. This prevents identification of small structures, and is again consistent with the conventional NMR observations for these soils (Table 1). All other native soils depicted in Fig. 2 and Fig. 3 provided excellent plant root images that were typically superior in quality to those acquired from any of the artificial soils in Fig. 1. Unlike some artificial soils, none of the native soils exhibited detectable background signals from soil water, despite a water content range of 9 to 190 g kg^{-1}. Images acquired from root systems in duplicate pots of these soils gave comparable results, except for a Kinston loamy sand sample whose image revealed signal losses near the hypogeal cotyledon and near the emerging stem (Fig. 4). Two ~3-mm lengths of ferromagnetic wire found at the corresponding locations in the pot were identified as the cause of these image artifacts.

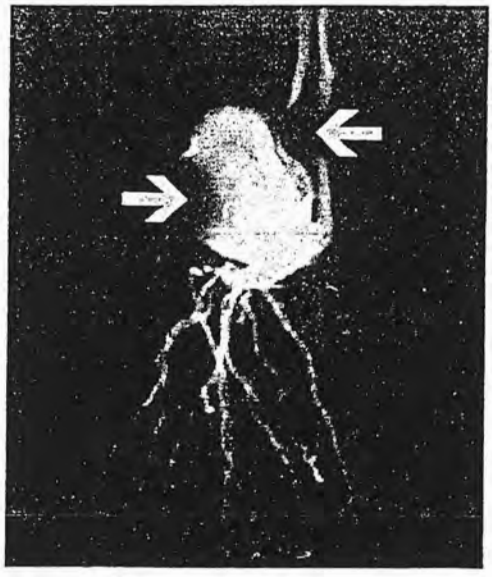

Fig. 4 ^{1}H NMR image of a second 30-day-old *V. faba* seedling root system in Kinston loamy sand at 113 g kg^{-1} water content. NMR signal distortion and loss on the left side of the cotyledon and on the right in the emerging stem was caused by the presence of two ~3-mm lengths of ferromagnetic wire located as indicated by the white arrows. (Scale 1:1.7.)

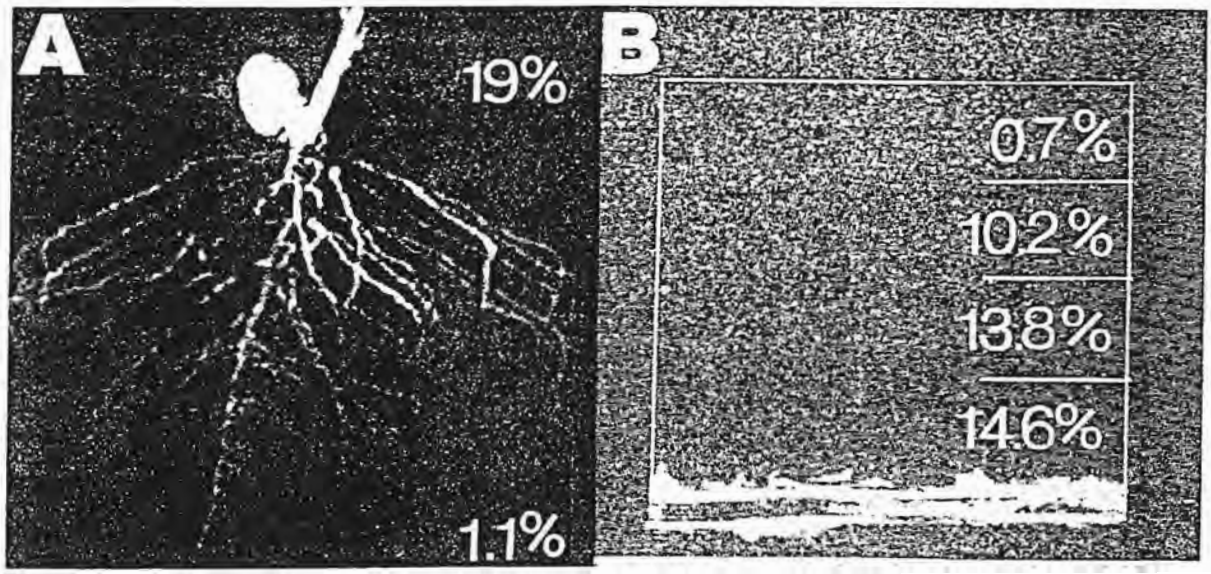

Fig. 5 A. ^{1}H NMR image of a recently watered *V. faba* root system in Lucy loamy sand with a soil water gradient ranging from 19% (190 g kg^{-1}) at the level of the cotyledon to 1.1% (11 g kg^{-1}, bottom) at the level of the taproot. Soil water is only faintly visible at the top. B. ^{1}H NMR image of a 1-L beaker containing four homogeneous layers of Eustis loamy fine sand at 0.7, 10.2, 13.8 and 14.6% (7, 102, 138, and 146 g kg^{-1}) water contents as labeled. The outline of the beaker is shown in white; lines to the right mark the location of 6-mm-thick disc of Styrofoam that separated the soil layers. No NMR signals are detectable from soil water relative to background level, except at the base where free water has moved downward to the Styrofoam disc supporting it. (Scale 1:1.7.)

Root system images in Fig. 2(B–G) and Fig. 3 accurately reproduced the root structures extricated from the soils by washing, notwithstanding damage sustained during the retrieval process. The root system image in Wynnville fine sandy loam (Fig. 2B) shows an overall deterioration that was confirmed on extrication. A dark irregular area visible on the cotyledons was found to be diseased tissue caused by the saprophytic fungus, *Cunninghamella elegans* Lendner. The smallest roots that could be identified in images were 0.3 mm. In Lakeland sand (Fig. 2E). the taproot did not develop, perhaps because of injury at transplant, and a small root system resulted. In Blanton loamy sand (Fig. 2G), bright irregular spots evident in the images at some of the root meristems were found to be enlarged and stubby upon extrication. Measurements of soil pH at 4.6 and Al and Ca levels at 162 and 59 mg kg^{-1}, respectively, implicated Al toxicity as the most likely cause. The root system in Eustis fine sandy loam (Fig. 3) has a distinct dotting pattern toward its center. This was due to an unidentified pathogen that produced alternating bands of healthy and necrotic zones along the roots. The sudden downward turn of long lateral roots in Lucy loamy sand and Kinston loamy sand (Fig. 2C,F) is the result of peripheral contact with the pot walls.

To further investigate the visibility of soil water in ^{1}H NMR images from those natural soils that were conducive to plant root imaging, imaging was repeated on potted seedlings following the addition of water, and on beakers containing segregated layers of soils with different water contents. Figure 5A is an image of the Lucy loamy sand seedling with a soil water content gradient from 190 g kg^{-1} (mud) at the top of the pot to 11 g kg^{-1} at the bottom of the pot where the taproot ends. To create this condition, a 12.5-mm "rain" was applied to the pot surface by light uniform spraying. Only a faint shadow of NMR signal is detectable at the very top. Figure 5B shows a layered beaker (1-L, glass) of Eustis fine sandy loam samples with water contents from 7 to 146 g kg^{-1}. These values correspond to soil water potentials of approximately -1500 and -9 kPa based on texture (total sand 73%, clay 6%, silt 21%; and fine sand 41%; all are percent of total soil) and the regression equations of Puckett et al. (12). The beaker was prepared by stacking four thin plastic bags of soil; into the bottom of each bag had been placed a 6-mm-thick disc of Styrofoam; samples were thereby conformed into discrete cylindrical volumes of soil. No soil water NMR signals could be detected above background noise. Bright signals at the base of this beaker derive not from the 146 g kg^{-1} soil sample, but from free water that moved from this sample to the Styrofoam disc below.

Similarly, a *V. faba* seedling in Eustis fine sandy loam at 146 g kg^{-1} water was clearly imaged without background signals from soil water (image not shown). At 146 g kg^{-1}, the amount of water in a 1-mm-thick cross section of a 150-mm pot of Eustis loamy fine sand is of the order 30-fold that which is present in a 1-mm root, assuming a root water content of 800 g kg^{-1} (19). Thus, in NMR images of Eustis fine sandy loam, NMR signal contributions from soil water were attenuated by a factor of greater than 30, relative to the NMR signal contributions from root water.

DISCUSSION

Currently, all plant root NMR imaging is performed on instruments ostensibly devoted to medical or animal research. Since machine time is at a premium at facilities conducting this research, the development of simple screening procedures that permit preselection of soil substrates to yield optimum NMR image quality is often crucial to the success of a plant root imaging experiment, eliminating months of effort in cultivating

experimental plants in unsuitable media. The present study suggests that conventional NMR tests of soil samples for ^1H NMR signals derived from water-containing capillaries embedded therein provide a reliable and rapid indication of soil suitability for root imaging studies, notwithstanding the random occurrence of ferromagnetic particles as was apparent in the second Kinston loamy sand sample (Fig. 4).

While no soils with magnetic fractions greater than about 4% produced suitable plant root images, no obvious correlation between soil magnetic fraction and signal observation in the conventional NMR study or NMR image quality was evident amongst specimens with magnetic fractions less than 4%. Thus, other factors unrelated to soil ferromagnetic particle content must have been responsible for the variability in NMR imaging performance of these soils. Since the RF magnetic field is the only other requisite agent for conventional NMR, and the visibility of NMR signal in the conventional NMR experiment correlated well with the success of the imaging studies, variability in RF magnetic field penetration is the most probable cause of differences in the NMR performance of soils with low magnetic fractions.

Perhaps the most surprising and potentially useful findings of the present study were the invisibility of soil water in native soils over an extremely broad range of water contents, and the superior NMR performance of some of the natural soils compared to artificial substrates. The results are valuable because, for the first time, they demonstrate that root systems grown in naturally occurring soil series are accessible to ^1H NMR imaging. Furthermore, the visibility of root water against a background of invisible soil water in NMR images from native soils provides excellent root-to-soil image contrast.

This fortuitous inability of ^1H NMR imaging to detect soil water when soil water is known to be the dominant source of protons in a pot is likely attributable to a shortened NMR T_2 relaxation of water in soil, presumably owing to the adsorption of water molecules onto the surface of soil particles yielding a more rigidly bound system than that of NMR-visible water molecules in roots.[3]. The attenuation of NMR signals from soil water, by factors of 30 or more by T_2 processes, as observed in Eustis fine sandy loam, would require T_2 values of less than 6 ms, given the 20-ms spin echo used in the NMR imaging pulse sequence. Conversely, the occurrence in NMR images of significant soil water signals in the artificial soils even at relatively low soil water contents suggests that the water is less rigidly bound at the molecular level than in the native soils, and that the T_2 values are correspondingly longer. This is not inconsistent with the greater water-bearing capacity of the artificial soils. Clearly, differences in the bound state of water in various agricultural soils and their effects, if any, on the accessibility of water to plant root systems are of themselves a worthy subject for further investigation by ^1H NMR. For future work it will be essential to consider soil texture, porosity, water potential, and solution chemistry.

In conclusion, ^1H NMR imaging is a practical and currently unique tool for studying plant root systems in many artificial and natural soil media, nondestructively in situ. Examination of soil samples by conventional NMR provides a more reliable test of the suitability of soils for imaging studies than do measurements of the ferromagnetic particle content alone. Nuclear magnetic resonance signals from soil water do not necessarily interfere with signals from roots in images, and in the case of the natural soils studied, soil water was rendered largely invisible up to near saturation. This means that cores from the field or plants at any stage of a water stress cycle can be examined. Root diseases can often be detected in images.

ACKNOWLEDGMENTS

We thank A.R. Mitchell, B.F. Hajek, F.A. Johnson, J.H. Shinn, and R.W. Redington for fruitful discussion and support; J.N. McCrimmon and J.A. Batchelor for technical assistance; E.A. Curl, G. Morgan-Jones, and M.D. Freeman for microbiological identification; and G.L. Rome for editorial comments. Partial support from the Carbon Dioxide Research Division, Office of Basic Energy Sciences, U.S. Department of Energy, through Interagency no. DEAI-01-86ER60001 to the USDA, and from the Plant Ecology Group, Environmental Sciences Division, Lawrence Livermore National Laboratory, is acknowledged.

REFERENCES

1. Bohm, W., L. Kutschera, and E. Lichtenegger (ed.) 1983. Wurzelokologie und ihre nutzanwendung/Root ecology and its practical application. Verlag Bundesanstalt fur alpenlandische Landwirtschaft, Gumpenstein, Austria.
2. Bohm., 1979. Methods of studying root systems. Springer-Verlag, Berlin, Germany.
3. Bottomley, P.A., H.R. Hart, W.A. Edelstein, J.F. Schenck, L.S. Smith, O.M. Mueller, and R.W. Redington. 1984. Anatomy and metabolism of the normal human brain studied by magnetic resonance at 1.5 tesla. Radiology (Easton, PA) 150:441–446.
4. ———, H.H. Rogers, and T.H. Foster. 1986. Nuclear magnetic resonance imaging shows water distribution and transport in plant root systems *in situ*. Proc. Natl. Acad. Sci. USA 83:87–89.
5. Brown, D.A., and Anwar-UL-Haq. 1984. A porous membrane-root culture technique for growing plants under controlled soil conditions. Soil Sci. Soc. Am. J. 48:692–695.
6. Curl, E.A., and B. Truelove. 1986. The rhizosphere. Springer-Verlag, Berlin, Germany.
7. Dugas, W.A., D.R. Upchurch, and J.T. Ritchie. 1985. A weighing lysimeter for evapotranspiration and root measurements. Agron. J. 77:821–825.
8. Fukushima, E., and S.B.W. Roeder. 1981. Experimental pulse NMR: A nuts and bolts approach. Addison-Wesley Publishing Company, Inc. Reading, Massachusetts.
9. Hainsworth, J.M., and L.A.G. Aylmore. 1986. Water extraction by single plant roots. Soil Sci. Soc. Am. J. 50:841–848.
10. Mansfield, P., and P.G. Morris. 1982. NMR imaging in biomedicine. Academic Press, New York.
11. Ottman, M.J., and H. Timm. 1984. Measurement of viable plant roots with the image analyzing computer. Agron. J. 76:1018–1020.
12. Puckett, W.E., J.H. Dane, and B.F. Hajek. 1985. Physical and mineralogical data to determine soil hydraulic properties. Soil Sci. Soc. Am. J. 49:831-n836.
13. Roberts, J.K.M. 1984. Study of plant metabolism *in vivo* using NMR spectroscopy. Annu. Rev. Plant Physiol. 35:375–386.
14. Robertson, B.M., A.E. Hall, and K.W. Foster. 1985. A field technique for screening for genotypic differences in root growth. Crop Sci. 25:1084–1090.
15. Rogers, H.H., P.A. Bottomley, and T.H. Foster. 1985. Application of nuclear magnetic resonance imaging to plant root studies. p. 1152–1157. *In* Proc. Int. Conf. on Soil Dynamics, vol. V., Auburn University, AL. Auburn University, Auburn University, AL.
16. Smith, S.L. 1985. Nuclear magnetic resonance imaging. Anal. Chem. 57:595A–608A.

17. Taylor, H.M., and S.T. Willatt. 1983. Shrinkage of soybean roots. Agron. J. 75:818–820.
18. Upchurch, D.R., and J.T. Ritchie. 1984. Battery-operated color video camera for root observations in mini-rhizotrons. Agron. J. 76:1015–1017.
19. Willatt, S.T., R.B. Struss, and H.M. Taylor. 1978. *In situ* root studies using neutron radiography. Agron. J. 70:581–586.
20. Witcofski, R.L., N. Karstaldt, and C.L. Partain. 1982. NMR imaging. The Bowman Gray School of Medicine, Wake Forest University, Winston-Salem, NC.